JKAU: Eng. Sci., **vol. 13 no. 2,** pp. 43-71 (1421 A.H. / 2001 A.D.)

Analysis of an AC-DC Full-controlled Converter Supplying Separately Excited DC Motor Parallel with Series DC Motor Loads

YUSUF A. Al-TURKI
MOHAMMED M. AL-HINDAWI and OBAID T. AL-SUBAIE
Department of Electrical and Computer Engineering,
King AbdulAziz University, Jeddah, Saudi Arabia

ABSTRACT. Controlled rectifiers are widely used as a source of DC motors power supply. It is important to study motor characteristics when fed from such converters. Early work has studied single motor characteristics when fed from a converter. This paper is concerned with the study of an AC-DC full-controlled converter supplying separately excited DC motor parallel with series DC motor loads. Continuous and discontinuous converter currents are considered. The critical firing angle is deduced. The margin firing angle that separates motor operation from generator operation of the separately excited machine is investigated. The performance characteristics have been derived and studied for each of: constant firing angle, constant torque of the separately excited motor and constant horsepower of the series motor. Waveforms for each load current and converter current are investigated for different modes of operation.

KEY WORDS: Controlled rectifiers, AC-DC converters, Full-controlled converters, Series motor, separately excited motor, Parallel loads.

1. Introduction

DC motors are found in many applications in our daily life. Such motors are heavily used in industrial processes, traction and elevators, entertainment "industry", toys and home appliances. Separately excited DC motor is used in applications requiring independent field control where field supply is separate from the armature supply. On the other hand, the series motor has both field and

armature windings connected in series. In this manner, armature supply controls both field and armature circuits. It is common in industry to fix more than one DC motor connected in parallel and fed from the same source. At present, solid state converters with high ratings are available. This led to the use of such converters in supplying DC motors from AC source. The most common method of converter control is the phase control. In this method, thyristor commutation is achieved by line commutation and, therefore, no additional circuitry is needed. This makes it simple, less expensive and it requires minimal maintenance[1].

Some researchers have studied converter performance connected to a passive load. Chung[2] presented a steady-state analysis of a two-branch resistance-inductance parallel circuit controlled by an AC switch. Al-Juhani[3] also made an analysis of an AC-DC converter supplying two-parallel inductive loads. Regarding the active load, Doradla and Sen[4] presented one of the early attempts to study solid state series motor drive. They made an evaluation of control schemes for thyristor-controlled DC motor[5]. Harmonics presented by a converter supplying a single-motor have also been studied[6]. Most of the work reported in the literature is related to converter supplying a single DC motor or two parallel passive loads.

In this paper, analysis of a phase-controlled (AC-DC full-controlled) converter feeding separately excited DC motor parallel with series DC motor loads of different parameters and speeds will be investigated. The steady-state analysis of this system will be obtained for each of the two modes of operation, (i.e. continuous and discontinuous converter current). An expression for the critical firing angle (at which the converter current changes from one mode to the other) will be deduced. The margin firing angle (that separates motor operation from generator operation of the separately excited machine) will be investigated. Performance characteristics such as input power factor, supply current distortion factor, torque-speed, and motor current ripple factors have been derived and studied for: constant firing angle, constant torque of the separately excited motor and constant horsepower of the series motor.

2. Steady State Analysis

The circuit under consideration is shown in Fig. 1, where S1, S2, S3, S4 are four power thyristors connected as a full converter. The sinusoidal voltage source is considered to have an rms value of V volts, frequency of $\omega/2\pi$ Hz and zero internal impedance. The load consists of a separately excited DC motor parallel with a series DC motor. The motor currents are controlled by changing the thyristors-firing angle. The supply current may be continuous or discontinuous depending on the firing angle, the load parameters, and motor speeds. Each of the two modes will be treated separately.

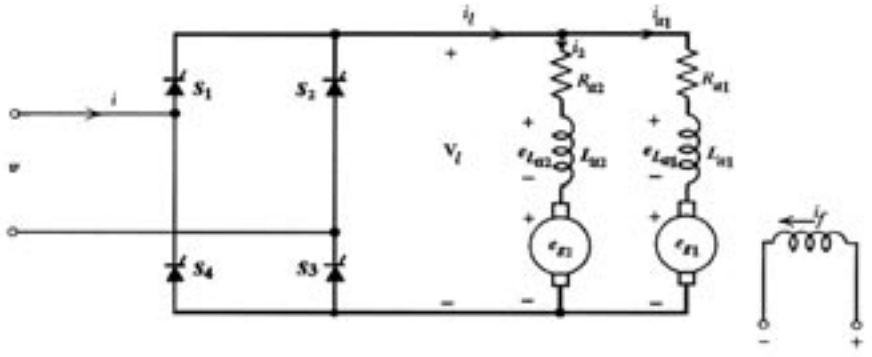

FIG. 1. Full controlled converter supplying separately excited DC motor parallel with series DC motor loads.

2.1 Continuous Mode

In this mode, the converter current i_l has a positive value at any instant of time. However, as the firing angle α increases, the value of i_l at $\omega t = \alpha$ decreases until it reaches zero value at the so-called critical firing angle α_c, Beyond α_c, the converter current will be discontinuous.

Throughout the period of $\alpha \leq \omega t \leq \pi + \alpha$, the voltage across each motor in the continuous mode is equal to the supply voltage assuming zero drops across thyristors. This means that for the separately excited DC motor:

$$\sqrt{2}V \sin \omega t = i_{c1} R_{a1} + L_{a1} \frac{d}{dt} i_{c1} + K_a \Phi N_1, \qquad \alpha \leq \omega t \leq \pi + \alpha \tag{1}$$

and for the series DC motor,

$$\sqrt{2}V \sin \omega t = i_{c2} R_{a2} + L_{a2} \frac{d}{dt} i_{c2} + K_{af2} i_{c2} N_2 + K_{res2} N_2, \quad \alpha \leq \omega t \leq \pi + \alpha \tag{2}$$

Where i_{c1} is the armature current of separately excited DC motor (i_{a1}) and i_{c2} is the armature current of series DC motor (i_{a2}) during the continuous mode.

During this mode, the converter current i_{cl} equals the supply current i_{cs} and is given by:

$$i_{cs} = i_{cl} = i_{c1} + i_{c2}, \qquad \alpha \leq \omega t \leq \pi + \alpha \tag{3a}$$

$$-i_{cs} = i_{cl} = i_{c1} + i_{c2}, \qquad \pi + \alpha \, \omega t \leq 2\pi + \alpha \tag{3b}$$

Separately Excited DC Motor Current

If steady-state speed and magnetic linearity are assumed, the solution of equation (1) is of the form:

$$i_{cl} = \sqrt{2}(V / Z_1)\sin(\omega t - \phi_1) + K_{c1}\, e^{(-(\omega t - a)/Q_1} - (K_a \Phi N_1 / R_1)(1 - e^{(-(\omega t - \alpha / Q_1)}) \qquad (4)$$

Where:

$R_1 = R_{a1}$, and $K_a \Phi$ is the constant of the separately excited DC motor, $Z_1 = \sqrt{R_1^2 + (\omega L_{a1})^2}$, $\phi_1 = \tan^{-1}(\omega L_{a1} / R_1)$, $Q_1 = \omega L_{a1} / R_1$, $K_{c1} = I_{c1} - \sqrt{2}(V / Z_1)\sin(\alpha - \phi_1)$, and I_{c1} is the initial value of i_{c1} at $\omega t = \alpha$.

Under steady state operation, i_{c1} at $\omega t = \alpha$ equals that at $\omega t = \pi + \alpha$ and is given by:

$$I_{cl} = -\sqrt{2}(V / Z_1)[1 + e^{(-\pi / Q_1)}) / (1 - e^{(-\pi / Q_1)})]\sin(\alpha - \phi_1) - (K_a \Phi N_1 / R_1). \qquad (5)$$

The ripple factor of i_{c1} is given by: $K_{cr1} = \sqrt{I_{c1rms}^2 / I_{c1av}^2 - 1}$. (6)

Where I_{c1av} and I_{c1rms} are the average and the rms values of the motor current respectively.

Full expressions for I_{c1av} and I_{c1rms} are given in Appendix [A].

Series DC Motor Current

If steady-state speed and magnetic linearity are assumed and the armature circuit resistance R_{a2} and inductance L_{a2} include the resistance and inductance of the series field winding, the solution of equation (2) is of the form:

$$i_{c2} = \sqrt{2}(V / Z_2)\sin(\omega t - \phi_2) + K_{c2}\, e^{(-(\omega t - \alpha)/Q_2)} - (K_{res2} N_2 / R_2)(1 - e^{(-(\omega t - \alpha)/Q_2)}) \qquad (7)$$

Where:

$R_2 = R_{a2} + K_{af2}\, N_2$, K_{af2} and K_{res2} are constants of the series motor, $Z_2 = \sqrt{R_2^2 + (\omega L_{a2})^2}$, $\phi_2 = \tan^{-1}(wL_{a2} / R_2)$, $Q_2 = \omega L_{a2} / R_2$, $K_{c2} = I_{c2} - \sqrt{2}$ $(V / V_2)\sin(\alpha - \phi_2)$, and I_{c2} is the initial value of i_{c2} at $\omega t = \alpha$.

Under steady state operation, i_{c2} at $\omega t = \alpha$ equals that at $\omega t = \alpha + \alpha$ and is given by:

$$I_{c2} = -\sqrt{2}(V / Z_2)[(1 + e^{(-\pi / Q_2)}) / (1 - e^{(-\pi / Q_2)})]\sin(\alpha - \phi_2) - (K_{res2} N_2 / R_2) \ . \qquad (8)$$

The ripple factor of i_{c2} is given by: $K_{cr2} = \sqrt{I_{c2rms}^2 / I_{c2av}^2 - 1}$. (9)

Where I_{c2av} and I_{c2rms} are the average and the rms values of the motor current respectively.

Full expressions for I_{c2av} and I_{c2av} are given in Appendix [A].

Critical Firing Angle

The critical firing angle α_c, which is the highest firing angle, for the continuous mode satisfies the condition of:

$$I_{c1} + I_{c2} = 0 \tag{10}$$

Therefore, the critical firing angle α_c is given from:

$$\alpha_c = \sin^{-1}[(A_1 C_1 \pm \sqrt{A_1^2 C_1^2 + (A_1^2 + B_1^2)(B_1^2 - C_1^2)})/(A_1^2 + B_1^2)] \tag{11}$$

Where:

$A_1 = F_1 \cos\phi_1 + F_2 \cos\phi_2$, $F_1 = -\sqrt{2}V / Z_1)\,(1 + e^{(-\pi/Q_1)})/(1 - e^{(-\pi/Q_1)})$,

$F_2 = -(\sqrt{2}V / Z_2)\,(1 + e^{(-\pi/Q_2)})/(1 - e^{(-\pi/Q_2)})$, $B_1 = F_1 \sin\phi_1 + F_2 \sin\phi_2$, and

$C_1 = (K_\alpha \Phi N_1 / R_1) + (K_{res2}\, N_2 / R_2)$.

Supply Current

The rms value of the fundamental component of the supply current is:

$$I_{cf} = \sqrt{a_{c1}^2 + b_{c1}^2 / 2} \tag{12}$$

And the phase angle of that component is given by:

$$\theta = \tan^{-1}\,(a_{c1} / b_{c1}) \tag{13}$$

Where a_{c1} and b_{c1} are the amplitudes of the cosine and sine fundamental components of i_{cs} respectively in the continuous mode.

The supply power factor is:

$$Pf = (I_{cf} / I_{csrms}) \cos\,\theta \tag{14}$$

And the supply current distortion factor is:

$$Df = I_{cf} / I_{csrms} \tag{15}$$

Where I_{csrms} is the rms value of the supply current.

Full expressions for I_{csrms} , a_{c1} , *and* b_{c1} are given in Appendix [A].

2.2 Discontinuous Mode

The discontinuous mode of operation occurs at a firing angles greater than α_c. In this mode, the converter current i_l increases from zero at $\omega t = \alpha$ to a maximum value and then decreases to become zero again at $\omega t = \beta$ which is referred to as the extinction angle. The angle β is, of course, less-than $\pi + \alpha$. Thus, the current i_{d1} is zero for $\beta \le \omega t \le \pi + \alpha$.

Detailed derivations of the currents in this mode of operation (conduction and non conduction periods) could be carried out in a manner similar to the continuous mode. Appendices [B&C] give such details.

The developed power and torque of the series DC motor are given by:

$$P_{motor} = K_{af}\ N_2\ I^2_{motor_{rms}}\ , \tag{16}$$

$$T_{motor} = K_{af}\ I^2_{motor_{rms}} \tag{17}$$

The developed power and torque of the separately excited DC motor are given by:

$$P_{motor} = K_a\ \Phi\ N_1\ I_{motor_{ava}}\ , \tag{18}$$

$$T_{motor} = K_a\ \Phi\ N_1\ I_{motor_{ava}}\ , \tag{19}$$

3. System Performance

In order to study the performance characteristics of the system under consideration, a computer program has been developed based on the equations derived in Section 3. The following data of load parameters are used[1]:

Separately exited	$R_{a1} = 0.6\ \Omega$.	Series DC motor :	$R_{a2} = 1.0\ \Omega$.
M1	$L_{a1} = 0.006\ h$.	M2	$L_{a2} = 0.012\ h$.
	$K_a\ \Phi = 0.55\ V.sec/rad.$		$K_{af2} = 0.027\ h$.
V = 120 volts			$K_{res2} = 0.0273\ V/rad/s.$

3.1 Critical Firing Angle

It is noted from Fig. 2 that, the critical firing angle α_c decreases as the speed of any motor or both is increased. The effect of changing M1 field current (or $K_a\Phi$) is shown in Fig. 3. The figure reveals that the critical firing angle α_c decreases as the value of $K_a\Phi$ is increased. Fig. 4 shows the operating regions of the separately excited DC motor. In this figure, there are two modes of operation (continuous and discontinuous). For the continuous mode there is a margin angle α_{mg} that separates motor operation from generation operation of the machine. For firing angle α higher than α_{mg} the machine acts as a generator. It is noticed that α_{mg} is constant in the continuous mode. This could be realized in view of equation (A-1), which shows that I_{1av} is independent of M2 parameters in the continuous mode. Since both $K_a\ \Phi$ and N1 are constants in Fig 4 then α_{mg} (at which I_{1av} = zero) is also constant. For the discontinuous mode, I_{1av} depends on the parameters of both motors as seen in equation (C-1). Therefore, changing N2 would effect α_{mg} leading to a variable α_{mg} in the discontinuous mode. The

intersection of α_c and α_{mg} curves divides the operation range into three distinctive modes normally:

1. Motor in the continuous mode.
2. Motor in the discontinuous mode.
3. Generator mode.

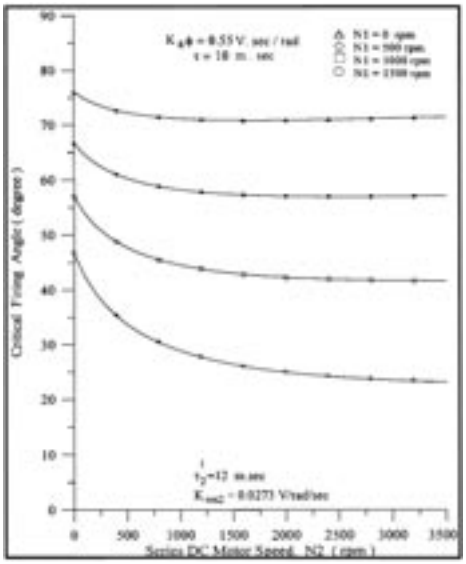

FIG. 2. Critical firing angle versus series DC motor speed N2 for different values of separately excited DC motor speed N1.

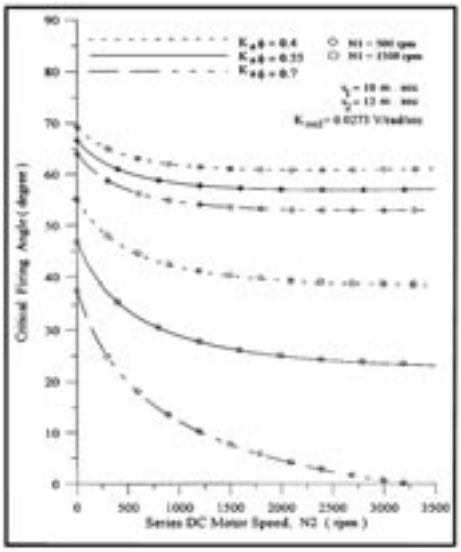

FIG. 3. Critical firing angle versus motor speed N2 for different values of $K_a \Phi$ and motor speed N1.

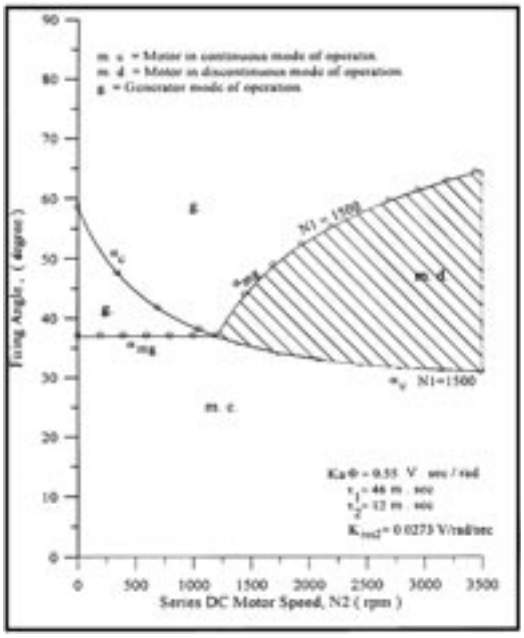

FIG. 4a. Operating regions of separately excited DC motor.

Figs 4b and 4c are given for different time constant of M1. It is clear that increasing τ_1 changes α_c which leads to an extended range of operation in the continuous mode.

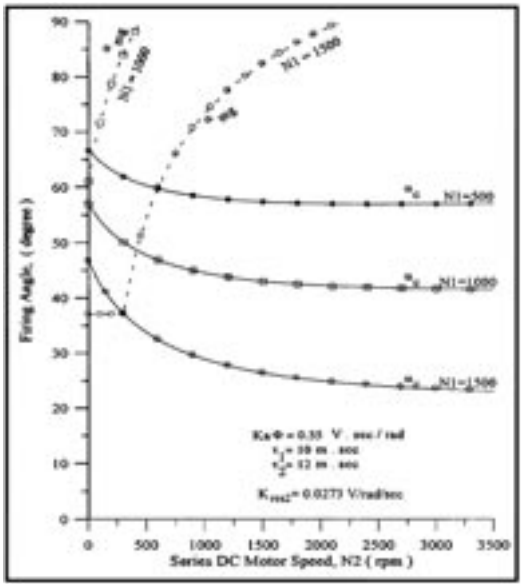

FIG. 4b. Operating regions of separately excited DC motor (τ_1 = 10 m.sec) for different values of motor speed N1.

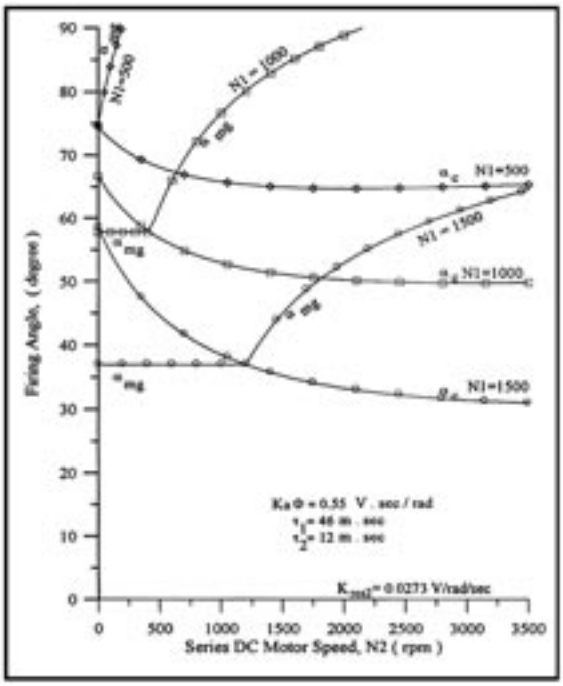

FIG. 4c. Operating regions of a separately excited DC motor (τ_1 = 46 m.sec) for different values of motor speed N1.

3.2 Current and Voltage Waveforms

The currents i_l, i_1 and i_2 are obtained using equations (3), (4) and (7) for the continuous mode and (B-3), (B-4), (B-6), (B-9) and (B-10) for the discontinuous mode. The continuous mode, critical firing angle, and discontinuous mode are shown in Figs. (5-7).

3.3 System Performance Parameters for Constant Torque Operation

It is seen from Fig. 8 that, the firing angle α decreases as the motor speed N1 is increased. At constant motors' speeds, the firing angle α increases as the torque level is decreased. The regions of discontinuous converter current are represented by dotted lines.

3.3.1 Supply Power Factor

When the separately excited DC motor is used for constant-torque applications, Fig. 9 shows that the supply power factor decreases with a decrease in either motor speed N1 or load torque.

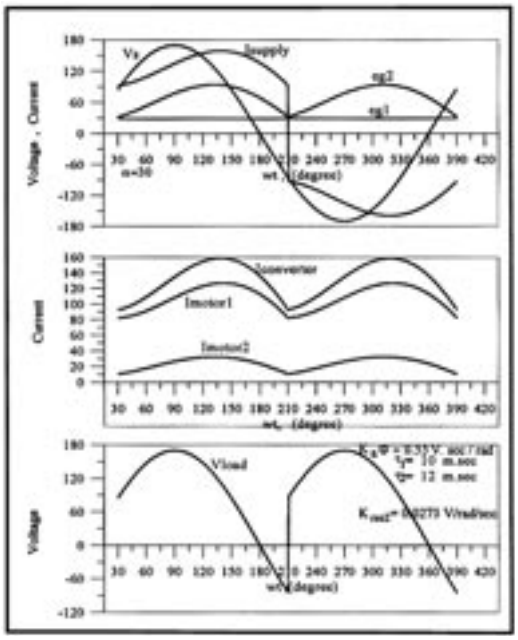

FIG. 5. Current and voltage waveforms in continuous converter current mode for N1 = 500 rpm, N2 = 1000 rpm, and $\alpha = 30^{\circ}$.

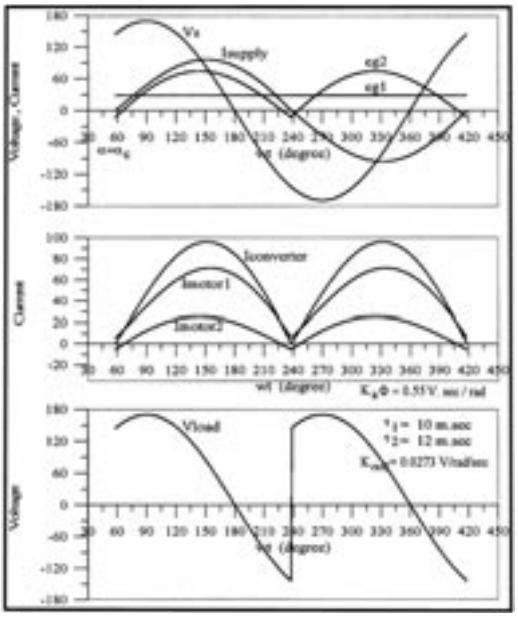

FIG. 6. Current and voltage waveforms in continuous converter current mode for N1 = 500 rpm, N2 = 1000 rpm, and $\alpha = \alpha_c = 58.2134^{\circ}$.

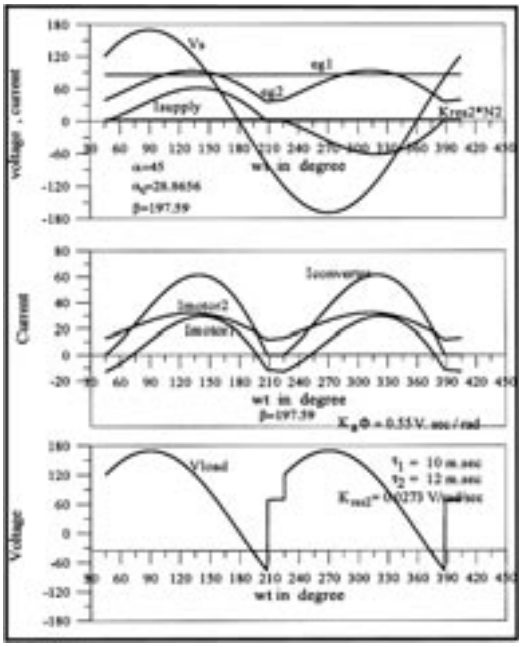

FIG. 7. Current and voltage waveforms in discontinuous converter current mode for N1 = 1500 rpm, N2 = 1000 rpm, and $\alpha = 45^{\circ}$.

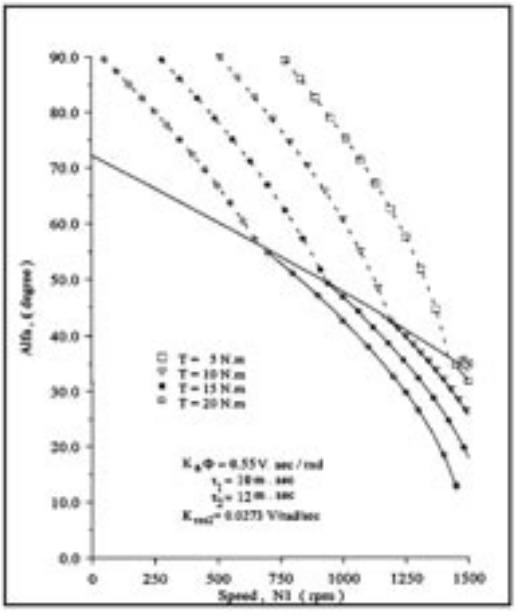

FIG. 8. Firing angle versus motor speed N1 for different values of torque level of M1, for N2 = 500 rpm.

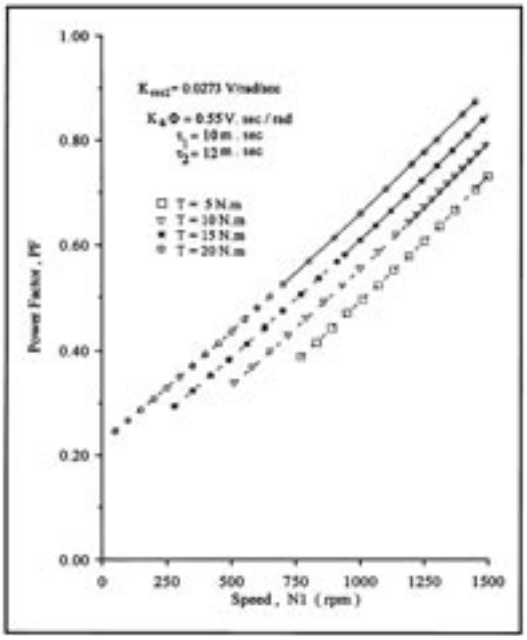

FIG. 9. Supply power factor versus motor speed N1 for different values of torque level of M1, for N2 = 500 rpm.

3.3.2 Supply Current Distortion Factor

Fig. 10 shows that for continuous converter current mode, the distortion factor decreases as motor speed N1 is increased. And for constant motors' speeds, the distortion factor increases as the load torque is decreased. Opposite conclusions have been obtained for the discontinuous converter current mode.

It is noted that the best value of the distortion factor is obtained when the firing angle is closest to the critical firing angle.

3.3.3 Motor Current Ripple Factor

It is evident from Fig. 11 that, the current ripple factor of M1 increases as the load torque is decreased keeping motors' speeds constant.

3.4 System Performance Parameters for Constant- HP Operation

Series motors are normally used for constant-horsepower applications. It is seen from Fig. 12 that the firing angle increases as the horsepower level of M2 is decreased keeping motors' speeds constant. The critical firing angle is also indicated.

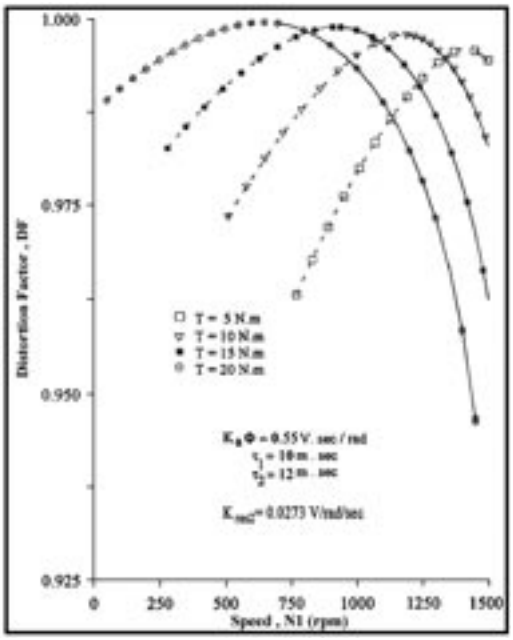

FIG. 10. Supply current distortion factor versus motor speed N1 for different values of torque level of M1, for N2 = 500 rpm.

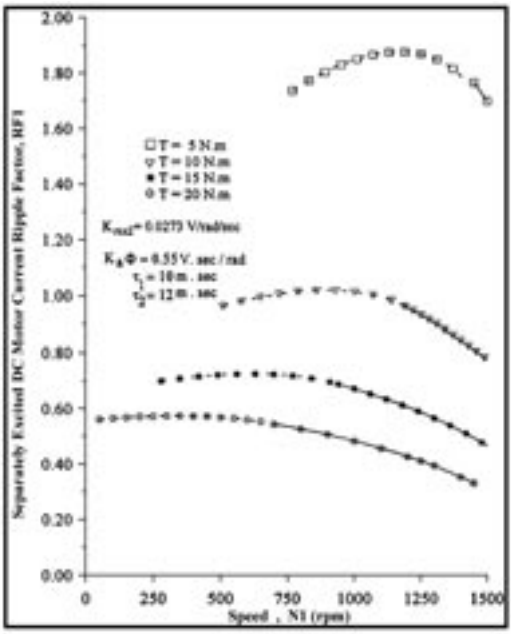

FIG. 11. Current ripple factor of motor one versus motor speed N1 for different values of torque level of M1, for N2 = 500 rpm.

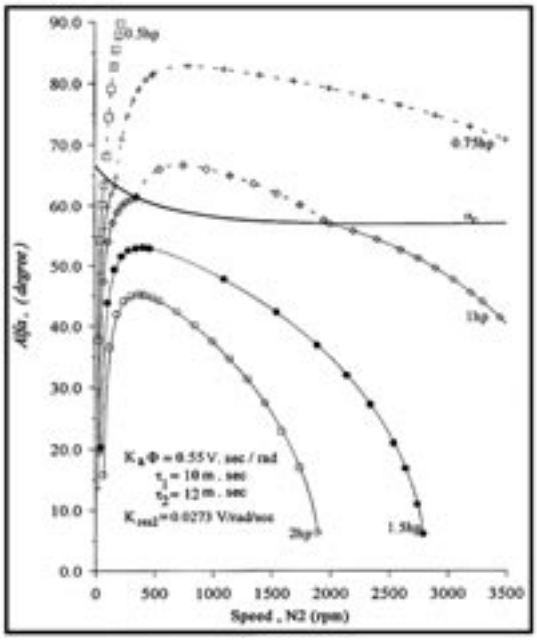

FIG. 12. Firing angle versus motor speed N2 for different values of horsepower level of M2, for N1 = 500 rpm.

3.4.1 Torque-speed characteristics

Fig. 13 shows that, the torque-speed characteristics of the series motor are drooping in nature. The system produces high torque at low speed and vice versa.

3.4.2 Supply Power Factor

It is evident from Fig. 14 that, the supply power factor decreases as the load horse power level of M2 is decreased keeping motors' speeds constant.

3.4.3 Motor Current Ripple Factor

According to Fig. 15, the current ripple factor of the series motor increases as the load horsepower level is decreased keeping motors' speeds constant.

3.5 System Performance Parameters for Constant Firing Angle, α, Operation

3.5.1 Separately Excited DC Motor Performance Parameters

a. Torque-Speed Characteristics: In Fig. 16 the dotted lines indicate discontinuous converter current. This figure shows that, as expected, the converter current is discontinuous at high values of the firing angle, α, and low values of torque.

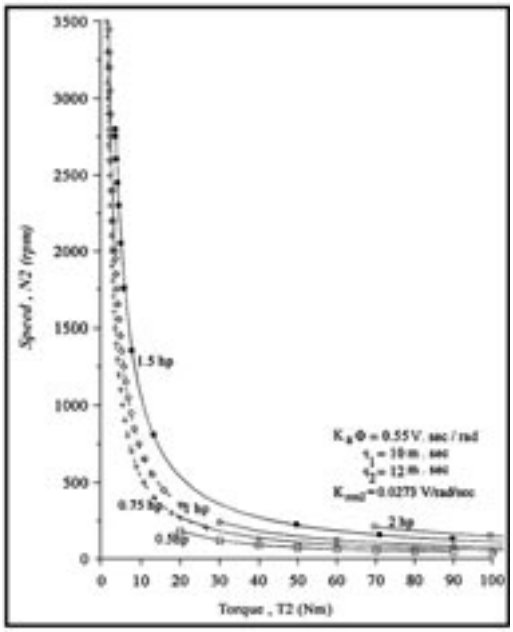

FIG. 13. Torque-speed characteristics (N2 versus T2) for different values of horsepower level of M2, for N1 = 500 rpm.

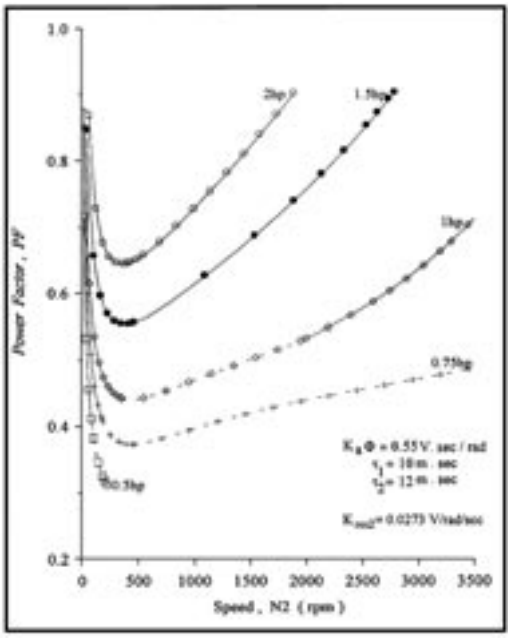

FIG. 14. Supply power factor versus motor speed N2 for different values of horsepower level of M2, for N1 = 500 rpm.

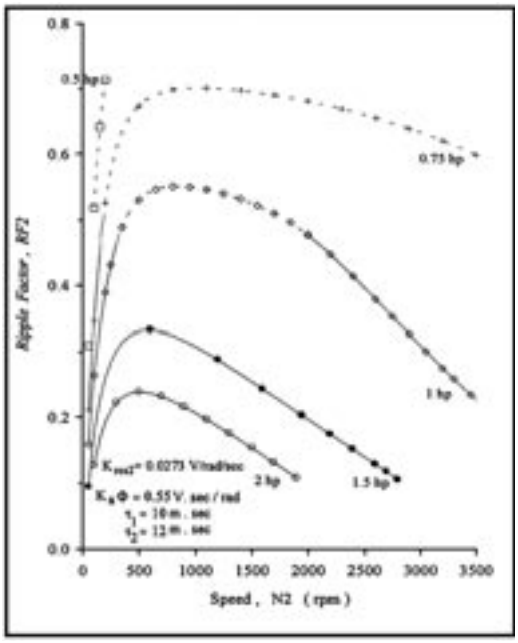

FIG. 15. Current ripple factor of motor two versus motor speed N2 for different values of horse-power level of M2, for N1 = 500 rpm.

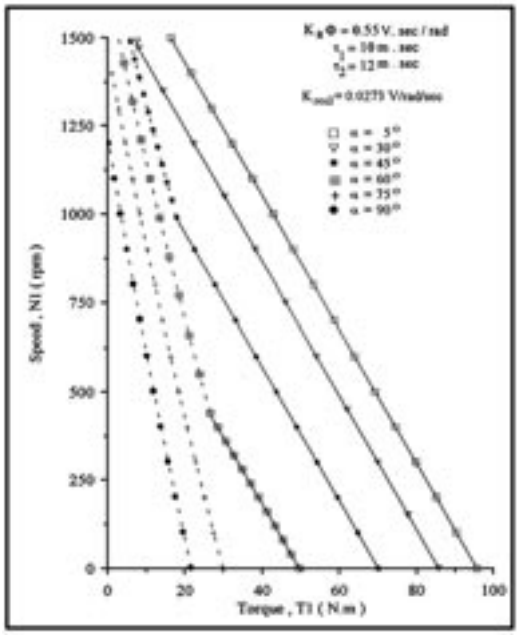

FIG. 16. Torque-speed characteristics (N1 versus T1) for different values of firing angle for N2 = 1000 rpm.

b. Supply Power Factor: Fig. 17 shows that, the supply power factor decreases as the firing angle is increased keeping motors' speeds constant.

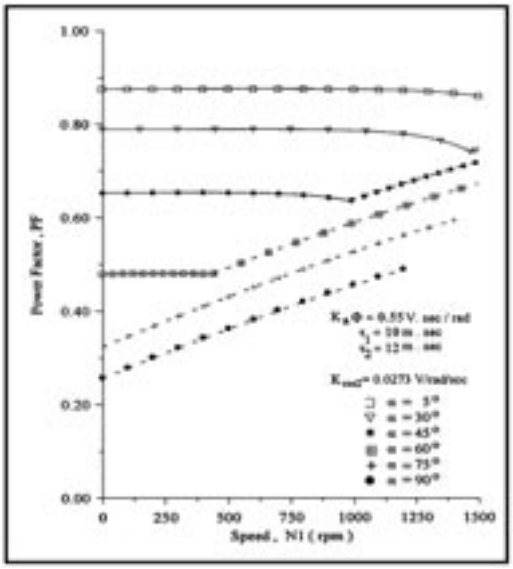

FIG. 17. Supply power factor versus motor speed N1 for different values of firing angle for N2 = 1000.

c. Motor Current Ripple Factor: It is evident from Fig. 18 that, the current ripple factor of M1 increases with the increase of either the firing angle or the motor speed N1.

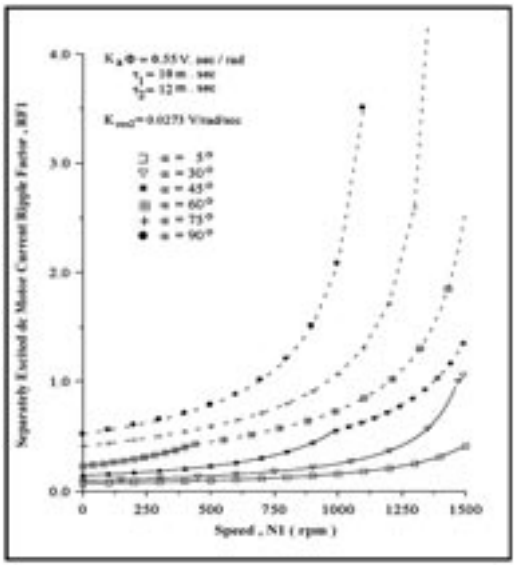

FIG. 18. Current ripple factor of motor one versus motor speed N1 for different values of firing angle, for N2 = 1000 rpm.

3.5.2 Series DC Motor Performance Parameters

a. Torque-Speed Characteristics: Fig. 19 shows that the torque-speed characteristics of the series motor are drooping in nature. As expected, the converter current is discontinuous at high values of the firing angle α, high speeds and low values of torque.

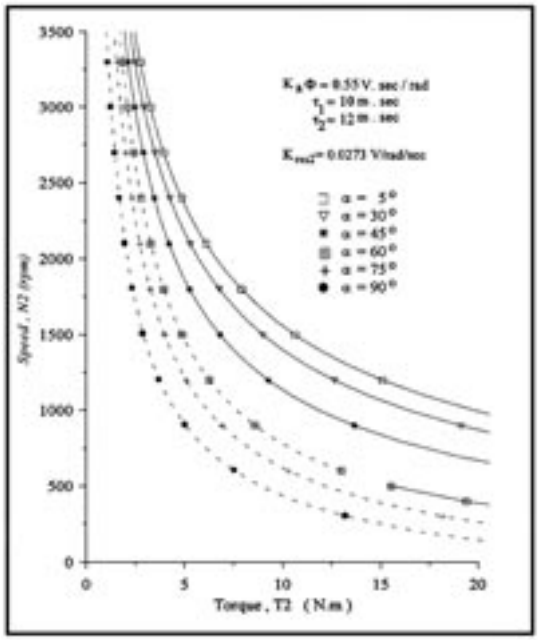

FIG. 19. Torque-speed characteristics (N2 versus T2) for different values of firing angle, for N1 = 500 rpm.

b. Supply Power Factor: It is evident from Fig. 20 that, the supply power factor decreases as the firing angle is increased keeping motors' speeds constant.

c. Motor Current Ripple Factor: It is evident from Fig. 21 that, the motor current ripple factor of M2 increases with the increase of either the firing angle or the motor speed N2. Comparison of ripple factors of Fig. 18 with those of Fig. 21 reveals that, for any value of firing angle and when N1 = N2, the ripple factor of the separately excited DC motor current is greater than the ripple factor of the series motor current.

4. Conclusion

In this paper, an AC-DC full-controlled converter supplying a separately excited DC motor parallel with a series DC motor has been investigated for steady-state operation. The margin firing angle, α_{mg}, that separates motor oper-

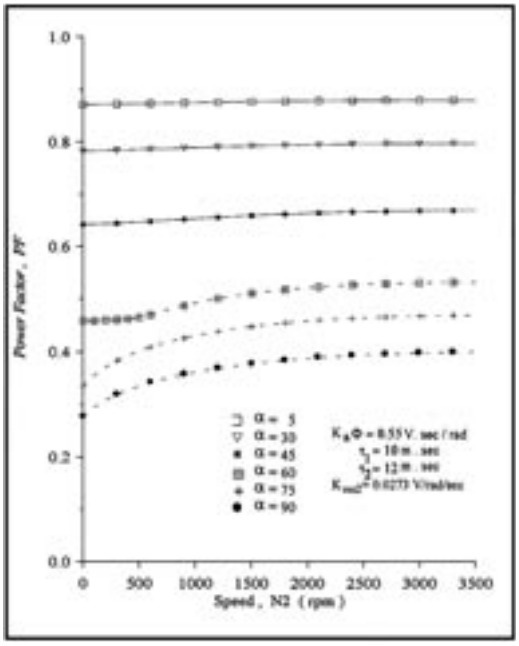

FIG. 20. Supply power factor versus motor speed N2 for different values of firing angle, for N1 = 500 rpm.

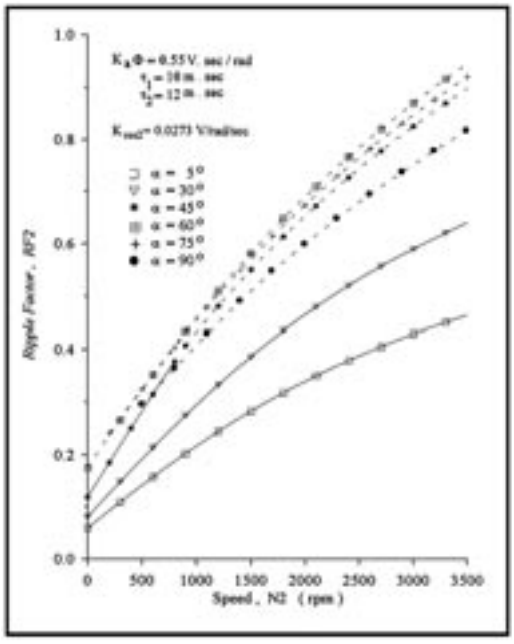

FIG. 21. Current ripple factor of motor two versus motor speed N2 for different values of firing angle, for N1 = 1000 rpm.

ation from generator operation of the separately excited machine has been studied. The following conclusions have been inferred:

4.1 Critical Firing Angle α_c

The critical firing angle α_c decreases as the speed of any motor or both is increased. However α_c increases as the field current of the separately excited motor is decreased. Increasing the time constant of any machine or both leads to an extended range of operation in the continuous mode.

4.2 Margin Firing Angle, α_{mg}

For the continuous converter current mode, α_{mg} is independent of the series motor parameters. For this mode, decreasing the separately excited motor speed, N1, leads to increase α_{mg}.

For the discontinuous converter current mode, α_{mg} depends on the parameters of both motors. For this mode, α_{mg} increases either by increasing the series motor speed, N2, or by decreasing the separately excited motor speed, N1.

4.3 Supply Current Distortion Factor

The best supply current distortion factor DF is obtained at α which is closest to α_c.

4.4 Constant Torque, T1, Operation

During this situation, α decreases and the input power factor PF increases as the motor speed N1 is increased.

4.5 Constant HP Operation, P2

During this situation, α decreases , the input PF increases and the motor current ripple factor RF2 decreases as the motor speed N2 is increased. Opposite conclusions have been obtained for very small values of N2.

4.6 Constant Speeds (N1 and N2) Operation

The increase in the value of torque, T1, leads to a lower α, higher power factor PF and a lower motor current ripple factor RF1. Decreasing the firing angle α increases the input power factor PF and decreases the motor current ripple factor. The decrease in the horsepower level of M2 leads to a higher α, lower input PF, and a higher motor current ripple factor RF2.

4.7 Constant Firing Angle α Operation

The increase in any motor speed leads to decrease of the torque level of that motor, small variation of PF for continuous converter current mode and increase the motor current ripple factor of the same motor. For any value of firing angle α and when N1 = N2, the ripple factor of the separately excited DC motor current is greater than the ripple factor of the series motor current.

References

[1] **Sen, P.C.,** *"Thyristor DC Drives"*, John Wiley, 1981.

[2] **Yung-Chung, Li,** "Steady-State Analysis of a Two Branch Resistance-Inductance Parallel Circuit Controlled by a Forced-Commutation Bidirectional AC Switch", *IEEE Transactions on Industrial Electronics and Control Instrumentation,* Nov. 1978.

[3] **Al-Johani, A.H.,** "Analysis of an AC-DC Converter Supplying Two Parallel Inductive Loads", *Master Thesis, King Abdulaziz University, S.A.,* 1987.

[4] **Doradla, S.R.** and **Sen, P.C.,** "Solid State Series Motor Drive", *IEEE Transactions on Industrial Electronics and Control Instrumentation,* May, 1975.

[5] **Sen, P.C.** and **Doradla, S.R.,** "Evaluation of Control Schemes for Thyristor-Controlled DC Motors", *IEEE Transactions on Industrial Electronics and Control Instrumentation,* August, 1978.

[6] **Kelley, A.W.** and **Yadusky, W.F.,** "Phase-Controlled Rectifier Line-Current Harmonics and Power Factor as a Function of Firing Angle and Output Filter Inductance", *IEEE Transactions on Industrial Electronics,* 1990.

[7] **Sen, P.C.,** "Electric Motor Drives and Control – Past, Present, and Future", *IEEE Transactions on Industrial Electronics,* 1990.

Appendix [A]

Continuous Mode

The avarage value of the separately excited DC motor current is obtained from: $I_{c1av} = (1/\pi) \int_{\alpha}^{\pi+\alpha} i_{c1} d\omega t$ and is given by:

$$I_{c1av} = 2\sqrt{2}(V/\pi Z_1)\cos(\alpha-\phi_1)+(K_{c1}Q_1/\pi)(1-e^{(-\pi/Q_1)}) \\ -(K_a\Phi N_1/R_1)[1-(Q_1/\pi)(1-e^{(-\pi/Q_1)})] \qquad (A-1)$$

And the rms value of the separately excited DC motor current is obtained from: $I_{c1rms} = \sqrt{(1/\pi)\int_{\alpha}^{\pi+\alpha} i_{c1}^2 d\omega t}$ and is given by:

$$I_{c1rms} = [(V^2/Z_1^2)+(K_{c1}+(K_a\Phi N_1/R_1))(2\sqrt{2}VQ_1^2/(\pi Z_1(1+Q_1^2))][(1/Q_1)\sin(\alpha-\phi_1) \\ +\cos(\alpha-\phi_1)](1+e^{(-\pi/Q_1)})-(4\sqrt{2}VK_a\Phi N_1/\pi Z_1R_1)\cos(\alpha-\phi_1) \\ +(Q_1/2\pi)(K_{c1}+(K_a\Phi N_1/R_1))^2(1-e^{(-2\pi/Q_1)})-(2Q_1K_a\Phi N_1/\pi R_1)(K_{c1} \\ +(K_a\Phi N_1/R_1))(1-e^{(-\pi/Q_1)})+(K_a\Phi N_1/R_1)^2]^{1/2} \qquad (A-2)$$

The average value of the series DC motor current is obtained from: $I_{c2av} = (1/\pi)\int_{\alpha}^{\pi+\alpha} i_{c2}\, d\omega t$ and is given by:

$$\begin{aligned} I_{c2av} &= 2\sqrt{2}(V/\pi Z_2)\cos(\alpha-\phi_2) + (K_{c2}Q_2/\pi)(1-e^{(-\pi/Q_2)}) \\ &\quad -(K_{res2}N_2/R_2)[1-(Q_2/\pi)(1-e^{(-\pi/Q_2)})] \end{aligned} \qquad (A-3)$$

And the rms value of the series DC motor current is obtained from: $I_{c2rms} = \sqrt{(1/\pi)\int_{\alpha}^{\pi+\alpha} i_{c2}^2\, d\omega t}$ and is given by:

$$\begin{aligned} I_{c2rms} = [&(V^2/Z_2^2) + (K_{c2} + (K_{res2}N_2/R_2))(2\sqrt{2}VQ_2^2/(\pi Z_2(1+Q_2^2)))[1/Q_2) \\ &\sin(\alpha-\phi_2) + \cos(\alpha-\phi_2)](1+e^{(-\pi/Q_2)}) - (4\sqrt{2}VK_{res2}N_2/\pi Z_2 R_2) \\ &\cos(\alpha-\phi_2) + (Q_2/2\pi)(K_{c2} + (K_{res2}N_2/R_2))^2(1-e^{(-2\pi/Q_2)}) \\ &-(2Q_2K_{res2}N_2/\pi R_2)(K_{c2} + (K_{res2}N_2/R_2))(1-e^{(-\pi/Q_2)}) \\ &+(K_{res2}N_2/R_2)^2]^{1/2} \end{aligned} \qquad (A-4)$$

The rms value of the supply current is obtained as:

$$I_{csrms} = \sqrt{(1/\pi)\int_{\alpha}^{\pi+\alpha} i_{cs}^2 d\omega t} = \sqrt{I_{c1rms}^2 + I_{c2rms}^2 + (1/\pi)\int_{\alpha}^{\alpha+\alpha} 2i_{c1}i_{c2}\, d\omega t} \qquad (A-5)$$

It could be shown that rms value of supply current is given by:

$$I_{csrms} = \sqrt{I_{c1rms}^2 + I_{c2rms}^2 + A + B + C + D + E + F + G + H + I + J} \qquad (A-6)$$

Where:

$A = (2V^2/Z_1Z_2)\cos(\phi_2-\phi_1)$,

$B = (2Q_1Q_2/\pi(Q_1+Q_2))(K_{c1} + (K_a\Phi N_1/R_1))(K_{c2} + (K_{res2}N_2/R_2))(1-e^{(-\pi(Q_1+Q_2)/Q_1Q_2)})$,

$C = (2\sqrt{2}VQ_2^2/\pi Z_1(1+Q_2^2))(K_{c2} + (K_{res2}N_2/R_2))((1/Q_2)\sin(\alpha-\phi_1) + \cos(\alpha-\phi_1))(1+e^{(-\pi/Q_2)})$,

$D = (2\sqrt{2}VQ_1^2/\pi Z_2(1+Q_1^2))(K_{c1} + (K_a\Phi N_1/R_1))((1/Q_1)\sin(\alpha-\phi_2) + \cos(\alpha-\phi_2))(1+e^{(-\pi/Q_1)})$,

$E = (-4\sqrt{2}V/\pi Z_2)(K_a\Phi N_1/R_1)\cos(\alpha-\phi_2)$,

$F = (-4\sqrt{2}V/\pi Z_1)(K_{res2}N_2/R_2)\cos(\alpha-\phi_1)$,

$G = (-2Q_1/\pi)(K_{c1}(K_{res2}N_2/R_2) + (K_a\Phi N_1/R_1)(K_{res2}N_2/R_2))(1-e^{(-\pi/Q_1)})$,

$H = (-2Q_2/\pi)(K_{c2}(K_a\Phi N_1/R_1) + (K_a\Phi N_1/R_1)(K_{res2}N_2/R_2))(1-e^{(-\pi/Q_2)})$, and

$J = 2(K_a\Phi N_1/R_1)(K_{res2}N_2/R_2)$

And a_{c1} and b_{c1} are the amplitudes of the cosine and the sine fundamental components of i_{cs} respectively and are given by: $a_{c1} = (1/\pi)\int_{\alpha}^{2\pi+\alpha} i_{cs}\cos\omega t d\,\omega t$, and is obtained from:

$$a_{c1} = -(\sqrt{2}V/Z_1)\sin\phi_1 + (2\varrho_1^2/(1+\varrho_1^2)\pi)(K_{c1} + (K_a\Phi N/R_1))((1/\varrho_1)\cos\alpha - \sin\alpha)(1+e^{(-\pi/\varrho_1)})$$
$$+(4K_a\Phi N_1/\pi R_1)\sin\alpha - (\sqrt{2}V/Z_2)\sin\phi_2 + (2\varrho_2^2/(1+\varrho_2^2)\pi)(K_{c2} \quad \text{(A –7)}$$
$$+(K_{res2}N_2/R_2))((1/\varrho_2)\cos\alpha - \sin\alpha)(1+e^{(-\pi/\varrho_2)}) + (4K_{res2}N_2/\pi R_2)\sin\alpha$$

And $b_{c1} = (1/\pi)\int_{\alpha}^{2\pi+\alpha} i_{cs}\sin\omega t d\,\omega t$, and is obtained from:

$$b_{c1} = (\sqrt{2}V/Z_1)\cos\phi_1 + (2\varrho_1^2/(1+\varrho_1^2)\pi)(K_{c1} + (K_a\Phi N/R_1))((1/\varrho_1)\sin\alpha + \cos\alpha)$$
$$(1+e^{(-\pi/\varrho_1)}) - (4K_a\Phi N_1/\pi R_1)\cos\alpha + (\sqrt{2}V/Z_2)\cos\phi_2 + (2\varrho_2^2/(1+\varrho_2^2)\pi)(K_{c2} + \quad \text{(A – 8)}$$
$$(K_{res2}N_2/R_2))((1/\varrho_2)\sin\alpha + \cos\alpha)(1+e^{(-\pi/\varrho_2)}) - (4K_{res2}N_2/\pi R_2)\cos\alpha$$

Appendix [B]

Discontinuous Mode

Conduction Period of the Discontinuous Mode

Throughout the period $\alpha \le \omega t \le \beta$, the load voltage is equal to the supply voltage. This means that for the separately excited DC motor:

$$\sqrt{2V}\sin\omega t = i_{d1}R_{a1} + L_{a1}\frac{d}{dt}i_{d1} + K_a\,\Phi\,N_1\ , \quad \text{(B – 1)}$$

and for the series DC motor:

$$\sqrt{2V}\sin\omega t - i_{d2}R_{a2} + L_{a2}\frac{d}{dt}i_{d2} + K_{af2}\,i_{d2}N_2 + K_{res2}N_2 \quad \text{(B – 2)}$$

Where: i_{d1} is the armature currents (i_{a1}) of the separately excited DC motor and i_{d2} is the armature currents (i_{a2}) of the series DC motor during the discontinuous mode.

During $\alpha \le \omega t \le \beta$, of the converter current i_{dl} equals the supply current and is given by:

$$i_{ds} = i_{dl} = i_{d1} + i_{d2} \qquad \alpha \le \omega t \le \beta \quad \text{(B – 3(a))}$$
$$-i_{ds} = i_{dl} = i_{d1} + i_{d2} \qquad \pi + \alpha \le \omega t \le \pi + \beta \quad \text{(B – 3(b))}$$

Separately Excited DC Motor Current

The solution of equation (B – 1) is of the form:

$$i_{d1} = \sqrt{2}(V/Z_1)\sin(\omega t - \phi_1) + K_{d1}e^{(-(\omega t-\alpha)/\varrho_1)} - (K_a\Phi N_1/R_1)(1-e^{(-(\omega t-\alpha)/\varrho_1)}), \alpha \le \omega t \le \beta \quad \text{(B – 4)}$$

Where:

$$K_{d1} = I_{d1} - (\sqrt{2}V/Z_1)\sin(\alpha - \phi_1) \quad \text{(B – 5)}$$

And i_{d1} is the initial value of i_{d1} at $\omega t = \alpha$.

Series DC Motor Current

The solution of equation (B – 2) is of the form:

$$i_{d2} = \sqrt{2}(V/Z_2)\sin(\omega t - \phi_2) + K_{d2}e^{(-(\omega t-\alpha)/\varrho_2)} - (K_{res2}N_2/R_2)(1-e^{(-(\omega t-\alpha)/\varrho_1)}), \alpha \le \omega t \le \beta \quad \text{(B – 6)}$$

Where:

$$K_{d2} = I_{d2} - (\sqrt{2}V / Z_2)\sin(\alpha - \phi_2) \qquad (B-7)$$

And I_{d2} is the initial value of i_{d2} at $\omega t = \alpha$.

Non Conduction Period of the Discontinuous Mode

During the period $\beta \le \omega t \le \pi + \alpha$, the converter current is equal to zero, and $i_{d1} = -i_{d2}$. The motors are connected in parallel. Thus:

$$R_1 i_{d1} + L_{a1}\frac{d}{dt}i_{d1} + K_a \Phi N_1 = R_2 i_{d2} + L_{a2}\frac{d}{dt}i_{d2} + K_{res2}N_2, \qquad \beta \le \omega t \le \pi + \alpha \qquad (B-8)$$

Solving (B – 8), one obtains:

$$i_{d1} = (K_{res2}N_2 - K_a\Phi N_1)/(R_1 + R_2) + (I'_{d1} - (K_{res}N_2 - K_a\Phi N_1)/(R_1 + R_2))e^{(-(\omega t - \beta)/Q)} \qquad (B-9)$$

Similarly,

$$i_{d2} = (K_a\Phi N_1 - K_{res2}N_2)/(R_1 + R_2) + (I'_{d2} - (K_a\Phi N_1 - K_{res2}N_2)/(R_1 + R_2))e^{(-(\omega t - \beta)/Q)} \qquad (B-10)$$

Where: $Q = \omega(L_{a1} + L_{a2}) / (R_1 + R_2)$, and I'_{d1} is the initial value of i_{d1} at $\omega t = \beta$ and is given by:

$$I'_{d1} = (\sqrt{2}V / Z_1)\sin(\beta - \phi_1) + K_{d1}e^{(-(\beta-\alpha)/Q_1)} - (K_a\Phi N_1 / R_1)(1 - e^{(-(\beta-\alpha)/Q_1)}) \qquad (B-11)$$

and I'_{d2} is the initial value of i_{d2} at $\omega t = \beta$ and is given by:

$$I'_{d2} = (\sqrt{2}V / Z_2)\sin(\beta - \phi_2) + K_{d2}e^{(-(\beta-\alpha)/Q_2)} - (K_{res2}N_2 / R_2)(1 - e^{(-(\beta-\alpha)/Q_1)}) \qquad (B-12)$$

At $\omega t = \pi + \alpha$, i_{d1} equals I_{d1} , and i_{d2} equals I_{d2}. Therefore, from equations (B – 5), (B – 9), and (B – 11) one gets:

$$\begin{aligned} I_{d1} = {} & [((K_{res2}N_2 - K_a\Phi N_1)/(R_1 + R_2))(1 - e^{(-(\pi+\alpha-\beta)/Q)}) + (\sqrt{2}V / Z_1) \\ & (\sin(\beta - \phi_1) - \sin(\alpha - \phi_1)e^{(-(\beta-\alpha)/Q_1)})e^{(-(\pi+\alpha-\beta)/Q)} - (K_a\Phi N_1 / R_1) \\ & (1 - e^{(-(\beta-\alpha)/Q_1)})e^{(-(\pi+\alpha-\beta)/Q)}]/(1 - e^{(-(\beta-\alpha)/Q_1)}e^{(-(\pi+\alpha-\beta)/Q)}) \end{aligned} \qquad (B-13)$$

Similarly: from equations (B – 7), (B – 10), and (B – 12) one gets:

$$\begin{aligned} I_{d2} = {} & [((K_a\Phi N_1 - K_{res2}N_2)/(R_1 + R_2))(1 - e^{(-(\pi+\alpha-\beta)/Q)}) + (\sqrt{2}V / Z_2) \\ & (\sin(\beta - \phi_2) - \sin(\alpha - Q_2)e^{(-(\beta-\alpha)/Q_2)})e^{(-(\pi+\alpha-\beta)/Q)} - (K_{res2}N_2 / R_2) \\ & (1 - e^{(-(\beta-\alpha)/Q_2)})e^{(-(\pi+\alpha-\beta)/Q)}]/(1 - e^{(-(\beta-\alpha)/Q_2)}e^{(-(\pi+\alpha-\beta)/Q)}) \end{aligned} \qquad (B-14)$$

The extinction angle β is determined by the solution of the equation $I_{d1} = -I_{d2}$. (B – 15)

Full expressions for I_{d1av}, I_{d1rms} , I_{d2av} , and I_{d2rms} are given in Appendix [C].

Where I_{d1av} and I_{d1rms} and the average and the rms values of the separately excited DC motor current respectively, and I_{d2av} and I_{d2rms} are the average and the rms values of the series DC motor current respectively.

The ripple factor of I_{dl} is given by: $K_{dr1} = \sqrt{(I^2_{d1rms} / I^2_{d1av}) - 1}$ (B – 16)

The ripple factor of i_{d2} is given by: $K_{dr2} = \sqrt{(I_{d2rms}^2 / I_{d2av}^2) - 1}$ (B – 17)

The rms value of the fundamental component of the supply current is

$$I_{df} = \sqrt{(a_{d1}^2 + b_{d1}^2)/2} \quad \text{(B – 18)}$$

And the phase angle of that component is given by:

$$\theta = \tan^{-1}(a_{d1} / b_{d1}) \quad \text{(B – 19)}$$

Where: a_{d1} and b_{d1} are the amplitudes of the cosine and sine fundamental components of i_{cs} respectively in the conscontinous mode.

The supply power factor is:

$$Pf = (I_{df} / I_{dsrms}) \cos\theta \quad \text{(B – 20)}$$

And the supply current distortion factor is:

$$Df = I_{df} / I_{dsrms} \quad \text{(B – 21)}$$

Full expressions for I_{dsrms} , a_{d1} , and b_{d1} are given in Appendix [C].

Appendix [C]

Average and rms values of the currents in the discontinuous mode

The average value of the separately excited DC motor current is given by:

$$I_{d1av} = (1/\pi)\int_{\alpha}^{\pi+\alpha} i_{d1}\, d\omega t .$$

Therefore:

$$\begin{aligned} I_{d1av} = {} & (\sqrt{2}V / Z_1\pi)[\cos(\alpha-\phi_1) - \cos(\beta-\phi_1)] + (Q_1/\pi)(K_{d1} \\ & + (K_a\Phi N_1 / R_1))(1 - e^{(-(\beta-\alpha)/Q_1)}) + (K_a\Phi N_1 / R_1)((\alpha-\beta)/\pi) \\ & + ((K_{res2}N_2 - K_a\Phi N_1)/(R_1+R_2))((\pi+\alpha-\beta)/\pi) \\ & + (Q/\pi)(((K_{res2}N_2 - K_a\Phi N_1)/(R_1+R_2)) - I'_{d1})(e^{(-(\pi+\alpha-\beta)/Q)} - 1) \end{aligned} \quad \text{(C – 1)}$$

The rms value of the separately excited DC motor current is found to be:

$$I_{d1rms} = \sqrt{(1/\pi)\int_{\alpha}^{\pi+\alpha} i_{d1}^2\, d\omega t} .$$

Therefore:

$$\begin{aligned} I_{d1rms} = {} & \{(2V^2/\pi Z_1^2)[(\beta-\alpha)/2 + [\sin 2(\alpha-\phi_1) - \sin 2(\beta-\phi_1)]/4 \\ & + (2\sqrt{2}V/\pi Z_1)(K_a\Phi N_1/R_1)[\cos(\beta-\phi_1) - \cos(\alpha-\phi_1] \\ & + (2\sqrt{2}V/\pi Z_1)(Q_1^2/(1+Q_1^2))(K_{d1} + (K_a\Phi N_1/R_1))[e^{(-(\beta-\alpha)/Q_1)}(-(1/Q_1) \\ & \sin(\beta-\phi_1) - \cos(\beta-\phi_1)) + ((1/Q_1)\sin(\alpha-\phi_1) + \cos(\alpha-\phi_1))] \\ & - (Q_1/2\pi)(K_{d1} + (K_a\Phi N_1/R_1))^2(e^{(-2(\beta-\alpha)/Q_1)} - 1) + (Q_1/\pi)(2K_{d1}(K_a\Phi N_1/R_1) \end{aligned}$$

$$+2(K_a\Phi N_1/R_1)^2)(e^{(-(\beta-\alpha)/Q_1)}-1)+(K_a\Phi N_1/R_1)^2(\beta-\alpha)/\pi$$
$$+((K_{res2}N_2-K_a\Phi N_1)/(R_1+R_2))^2((\pi+\alpha-\beta)/\pi)$$
$$+(2Q/\pi)[((K_{res2}N_2-K_a\Phi N_1)/(R_1+R_2))^2-I'_{d1}((K_{res2}N_2-K_a\Phi N_1)$$
$$/(R_1+R_2))](e^{(-(\pi+\alpha-\beta)/Q)}-1)-(Q/2\pi)(((K_{res2}N_2-K_a\Phi N_1)$$
$$/(R_1+R_2))-I'_{d1})^2(e^{(-2(\pi+\alpha-\beta)/Q)}-1\}^{1/2} \quad \text{(C – 2)}$$

The average value of the series DC motor current is given by:

$$I_{d2av}=(1/\pi)\int_{\alpha}^{\pi+\alpha} i_{d2}\,d\omega t\ .$$

Therefore:

$$I_{d2av}=(\sqrt{2}V/Z_2\pi)[\cos(\alpha-\phi_2)-\cos(\beta-\phi_2)]+(Q_2/\pi)(K_{d2}$$
$$+(K_{res2}N_2/R_2))(1-e^{(-(\beta-\alpha)/Q_2)})+(K_{res2}N_2/R_2)((\alpha-\beta)/\pi)$$
$$+((K_a\Phi N_1-K_{res2}N_2)/(R_1+R_2))((\pi+\alpha-\beta)/\pi)$$
$$+(Q/\pi)(((K_a\Phi N_1-K_{res2}N_2)/(R_1+R_2))-I'_{d2})(e^{(-(\pi+\alpha-\beta)/Q)}-1) \quad \text{(C – 3)}$$

The rms value of the series DC motor current is found to be:

$$I_{d2rms}=\sqrt{(1/\pi)\int_{\alpha}^{\pi+\alpha} i_{d2}^2\,d\omega t}\ .$$

Therefore:

$$I_{d2rms}=\{(2V^2/\pi Z_2^2)[(\beta-\alpha)/2+[\sin 2(\alpha-\phi_2)-\sin 2(\beta-\phi_2)]/4]+(2\sqrt{2}V/\pi Z_2)$$
$$(K_{res2}N_2/R_2)[\cos(\beta-\phi_2)-\cos(\alpha-\phi_2)]+(2\sqrt{2}V/\pi Z_2)(Q_2^2/(1+Q_2^2))(K_{d2}$$
$$+(K_{res2}N_2/R_2))[e^{(-(\beta-\alpha)/Q_2)}(-(1/Q_2)\sin(\beta-\phi_2)-\cos(\beta-\phi_2))$$
$$+(1/Q_2)\sin(\alpha-\phi_2)+\cos(\alpha-\phi_2))]-(Q_2/2\pi)(K_{d2}+(K_{res2}N_2/R_2))^2$$
$$(e^{(-2(\beta-\alpha)/Q_2)}-1)+(Q_2/\pi)(2K_{d2}(K_{res}N_2/R_2)+2(R_{res2}N_2/R_2)^2)$$
$$(e^{(-(\beta-\alpha)/Q_2)}-1)+(K_{res2}N_2/R_2)^2(\beta-\alpha)/\pi+((K_a\Phi N_1-K_{res2}N_2)/R_1$$
$$+R_2))^2((\pi+\alpha-\beta)+(2Q/\pi)[((K_a\Phi N_1-K_{res2}N_2)/(R_1+R_2))^2$$
$$-I'_{d2}((K_a\Phi N_1-K_{res2}N_2)/R_1+R_2))](e^{(-(\pi+\alpha-\beta)/Q)}-1)-(Q/2\pi)(((K_a\Phi N_1$$
$$-K_{res2}N_2)/(R_1+R_2))-I'_{d2})^2(e^{(-2(\pi+\alpha-\beta)/Q)}-1)\}^{1/2} \quad \text{(C – 4)}$$

The value of the supply rms current is obtained from:

$$I_{dsrms}=\sqrt{(1/\pi)\int_{\alpha}^{\beta} i_{ds}^2\,d\omega t}\ . \quad \text{(C – 5)}$$

Thus:

$$I_{dsrms} = \sqrt{(1/\pi)\int_{\alpha}^{\beta} i_{d1}^2 d\omega t + (1/\pi)\int_{\alpha}^{\beta} i_{d2}^2 d\omega t + (1/\pi)\int_{\alpha}^{\beta} 2 i_{d1} i_{d2} d\omega t} \qquad \text{(C – 6)}$$

Then rms value of the supply current is found to be:

$$\begin{aligned}
I_{dsrms} = \{&(2V^2/\pi Z_1^2)[(\beta-\alpha)/2 + [\sin 2(\alpha-\phi_1) - \sin 2(\beta-\phi_1)]/4] + (2\sqrt{2}V/\pi Z_1) \\
&(K_a\Phi N_1/R_1)[\cos(\beta-\phi_1) - \cos(\alpha-\phi_1)] + (2\sqrt{2}V/\pi Z_1)(Q_1^2/(1+Q_1^2))(K_{d1} \\
&+(K_a\Phi N_1/R_1))[e^{(-(\beta-\alpha)/Q_1)}(-(1/Q_1)\sin(\beta-\phi_1) - \cos(\beta-\phi_1)) \\
&+((1/Q_1)\sin(\alpha-\phi_1) + \cos(\alpha-\phi_1))] - (Q_1/2\pi)(K_{d1} + (K_a\Phi N_1/R_1))^2 \\
&(e^{(-2(\beta-\alpha)/Q_1)} - 1) + (Q_1/\pi)(2K_{d1}(K_a\Phi N_1/R_1) + 2(K_a\Phi N_1/R_1)^2) \\
&(e^{(-(\beta-\alpha)/Q_1)} - 1) + (K_a\Phi N_1/R_1)^2(\beta-\alpha)/\pi + (2V^2/\pi Z_2^2)[(\beta-\alpha)/2 \\
&+[\sin 2(\alpha-\phi_2) - \sin 2(\beta-\phi_2)]/4] + (2\sqrt{2}V/\pi Z_2)(K_{res2}N_2/R_2)[\cos(\beta-\phi_2) \\
&-\cos(\alpha-\phi_2)] + (2\sqrt{2}V/\pi Z_2)(Q_2^2/(1+Q_2^2))(K_{d2} + (K_{res2}N_2/R_2)) \\
&[e^{(-(\beta-\alpha)/Q_2)}(-(1/Q_2)\sin(\beta-\phi_2) - \cos(\beta-\phi_2)) + ((1/Q_2)\sin(\alpha-\phi_2) \\
&+\cos(\alpha-\phi_2))] - (Q_2/2\pi)(K_{d2} + (= (K_{res2}N_2/R_2))^2(e^{(-2(\beta-\alpha)/Q_2)} - 1) \\
&+(Q_2/\pi)(2K_{d2}(K_{res2}N_2/R_2) + 2(K_{res2}N_2/R_2)^2)(e^{(-(\beta-\alpha)/Q_2)} - 1) \\
&+(K_{res2}N_2/R_2)^2(\beta-\alpha)/\pi + (2V^2/\pi Z_1 Z_2)\cos(\phi_2-\phi_1)(\beta-\alpha) - (V^2/\pi Z_1 Z_2) \\
&[\sin(2\beta-\phi_2-\phi_1) - \sin(2\alpha-\phi_2-\phi_1)] + (2\sqrt{2}V/\pi Z_2)(K_a\Phi N_1/R_1)[\cos(\beta-\phi_2) \\
&-\cos(\alpha-\phi_2)] + (2\sqrt{2}V/\pi Z_1)(K_{res2}N_2/R_2)[\cos(\beta-\phi_1) - \cos(\alpha-\phi_1)] \\
&+(2\sqrt{2}V/\pi Z_2)(Q_1^2/(1+Q_1^2))(K_{d1} + (K_a\Phi N_1/R_1))[e^{(-(\beta-\alpha)/Q_1)}(-(1/Q_1) \\
&\sin(\beta-\phi_2) - \cos(\beta-Q_2)) + ((1/Q_1)\sin(\alpha-\phi_2) + \cos(\alpha-\phi_2))] \\
&+(2\sqrt{2}V/\pi Z_1)(Q_2^2/(1+Q_2^2))(K_{d2} + (K_{res2}N_2/R_2))[e^{(-(\beta-\alpha)/Q_2)}(-1(1/Q_2) \\
&\sin(\beta-\phi_1) - \cos(\beta-\phi_1)) + ((1/Q_2)\sin(\alpha-\phi_1) + \cos(\alpha-\phi_1))] \\
&+(2Q_1Q_2/\pi(Q_1+Q_2))(K_{d1} + (K_a\Phi N_1/R_1))(K_{d2} + (K_{res2}N_2/R_2)) \\
&(1 - e^{(-(Q_1+Q_2)(\beta-\alpha)/Q_1Q_2)}) + (2Q_2/\pi)(K_a\Phi N_1/R_1)(K_{d2} + (K_{res2}N_2/R_2)) \\
&(e^{(-(\beta-\alpha)/Q_2)} - 1) + (2Q_1/\pi)(K_{res2}N_2/R_2)(K_{d1} + (K_a\Phi N_1/R_1)) \\
&(e^{(-(\beta-\alpha)/Q_1)} - 1) + (2/\pi)(K_a\Phi N_1/R_1)(K_{res2}N_2/R_2)(\beta-\alpha)\}^{1/2}
\end{aligned} \qquad \text{(C – 7)}$$

And a_{d1} and b_{d1} are the amplitudes of the cosine and sine fundamental components of i_{ds} respectively and are given by:

$$\begin{aligned} a_{d1} &= (\sqrt{2}V/2\pi Z_1)[\cos(2\alpha-\phi_1)-\cos(2\beta-\phi_1)-2(\beta-\alpha)\sin\phi_1] \\ &+2(Q_1^2/(\pi(1+Q_1^2)))(K_{d1}+(K_a\Phi N_1/R_1))[e^{(-(\beta-\alpha)/Q_1)}(-(Q_1)\cos\beta \\ &+\sin\beta)+((1/Q_1)\cos\alpha-\sin\alpha)]-(2K_a\Phi N_1/\pi R_1))(\sin\beta-\sin\alpha) \\ &+(\sqrt{2}V/2\pi Z_2)[\cos(2\alpha-\phi_2)-\cos(2\beta-\phi_2)-2(\beta-\alpha)\sin\phi_2] \\ &+2(Q_2^2/(\pi(1+Q_2^2)))(K_{d2}+(K_{res2}N_2/R_2))[e^{(-(\beta-\alpha)/Q_2)}(-(1/Q_2)\cos\beta \\ &+\sin\beta)+((1/Q_2)\cos\alpha-\sin\alpha)]-(2K_{res2}N_2/\pi R_2))(\sin\beta-\sin\alpha)\ , \end{aligned} \tag{C-8}$$

and

$$\begin{aligned} b_{d1} &= (\sqrt{2}V/2\pi Z_1)[\sin(2\alpha-\phi_1)-\sin(2\beta-\phi_1)+2(\beta-\alpha)\cos\phi_1] \\ &+2(Q_1^2/(\pi(1+Q_1^2)))(K_{d1}+(K_a\Phi N_1/R_1))[e^{(-(\beta-\alpha)/Q_1)}(-(1/Q_1)\sin\beta-\cos\beta) \\ &+((1/Q_1)\sin\alpha+\cos\alpha)]+(2K_a\Phi N_1/\pi R_1))(\cos\beta-\cos\alpha) \\ &+(\sqrt{2}V/2\pi Z_2)[\sin(2\alpha-\phi_2)-\sin(2\beta-\phi_2]+2(\beta-\alpha)\cos\phi_2] \\ &+2(Q_2^2/(\pi(1+Q_2^2)))(K_{d2}+(K_{res2}N_2/R_2))[e^{(-(\beta-\alpha)/Q_2)}(-(1/Q_2)\sin\beta-\cos\beta) \\ &+((1/Q_2)\sin\alpha+\cos\alpha)]+(2K_{res2}N_2/\pi R_2))(\cos\beta-\cos\alpha) \end{aligned} \tag{C-9}$$

تحليل مقوم محكوم (كامل التحكم) يغذي محركًا منفصل الإثارة على التوازي مع محرك مستمر

يوسف عبد العزيز التركي ، محمد مصطفى الهنداوي و عبيد تركي السبيعي
قسم الهندسة الكهربائية وهندسة الحاسبات ، جامعة الملك عبد العزيز
جـــــــدة – المملكة العربية السعودية

المستخلص . المقوّمات المحكومة تستخدم بكثرة كمصادر تغذية لمحركات التيار المستمر . ومن المهم دراسة خصائص المحركات المغذاة بهذه المقوّمات ، وكذا دراسة خصائص المقوّمات المغذية لهذه الأحمال . وقد اهتمت الدراسات المتاحة بدراسة خصائص محرك واحد عند تغذيته من مقوّم محكوم . وتهتم هذه الورقة بدراسة خصائص مقوم كامل التحكم عندما يغذي محركًا منفصل الإثارة على التوازي مع محرك مستمر . وقد تمت هذه الدراسة لكل من نسقي تيار المقوّم (نسق التيار المتصل ، ونسق التيار المتقطع). وقد تم تحديد قيمة زاوية الإشعال التي تفصل بين عمل الآلة منفصلة الإثارة كمحرك وبين عملها كمولد .

كما تم استنتاج ودراسة خصائص المقوّم المحكوم وخصائص المحركين وذلك عن : ثبات زاوية الإشعال ، ثبات عزم المحرك منفصل الإثارة وعند ثبات القدرة الحصانية للمحرك المستمر .

وللتوضيح قدم البحث نماذج من الأشكال الموجية للتيارات والفلطيات المختلفة ، تحت ظروف تشغيلية متنوعة .